ANALYSIS OF TAPERED VELOCITY AND TAPERED COUPLING COUPLERS

by Ary Syahriar

Submission date: 22-Oct-2020 08:44AM (UTC+0000)
Submission ID: 1422970180
File name: Analysis_of_Taperred_Velocity_-_ISSTIN.pdf (353.98K)
Word count: 3599
Character count: 18543

ANALYSIS OF TAPERED VELOCITY AND TAPERED COUPLING COUPLERS

Ary Syahriar [1,2]

[1]Agency for the Assessment and Application of Technology of the Republic of Indonesia
[2] Department of Electrical Engineering Faculty of Science and Technology
University of Al Azhar Indonesia, Jl. Sisingamangaraja, Jakarta 12110

E-mail: ary@inn.bppt.go.id, ary@uai.ac.id

Abstract - **A simple design method to suppress the sidelobes in the directional coupler-type light power splitters is presented. Couplers with variable differences along the guide axis and the evolution of propagation constant between the waveguides are investigated, and the optimum profiles of the variation of the propagation-constant difference are designed for desired given power responses. A number of filter functions are used to model a coupler with relax length requirements but fulfilling the sidelobes standard. It is found that Hamming filter function offers the best sidelobe and maximum length constrain.**

Keywords *- couplers, coupled mode theory, tapered coupler, mode evolution*

I. INTRODUCTION

Directional couplers are frequently used in a number of applications such as power dividers, wavelength selective and polarization splitters [1]. However, because of its interferometric behaviour, it requires a strict fabrication tolerance, especially when used as a switching device [2]. Additionally, in silica-on-silicon, directional coupler switches are impractical, because of the thermal crosstalk which occurs between the two closely adjacent waveguides.

To improve tolerances (and to suppress the sidelobes in the device's switch characteristics) several modified designs of coupler were proposed for Ti:$LiNbO_3$ devices. These include devices with tapered gap between the guides [2][3], tapered guide width or indices [4]-[6], and both tapered gap and tapered width [7]. A useful performance improvement was obtained, at the cost of a slight increase in length and switching voltage. However, there is another advantage. The use of a tapered gap makes these structures inherently more suitable for implementation as a silica-on-silicon device, since the waveguide separation may now be much larger in regions where a significant thermo-optic effect is desired.

Around this time, Silberberg et al. demonstrated a rather different hybrid X-junction switch, known as the 'digital switch', with a tolerance in fabrication and operational conditions [8]. It has a step-like switch response, which eliminates precise voltage control; even more usefully, it is insensitive to polarisation and wavelength. Following this, Syms et al. proposed an analogous 'digital directional coupler' with a similarly desirable switching characteristic. The design was based on a linear taper in guide width combined with a parabolic variation in guide separation [7]. As in the hybrid X-junction, the device's operation is dependent on the evolution of a single normal mode due to the gradual change in shape of the device with distance, rather than by the beating of two modes as in a conventional coupler. Power transfer occurs in the middle of the structure, where the gap is minimum and the two guides have equal width.

Xie et al. [9] of the Heinrich-Hertz-Institute, Berlin, fabricated prototype GaInAsP/InP devices to this design, using an e-beam writing system with 50 nm resolution to lay out the structure and

approximately the predicted performance was obtained. However, they showed that to get full power transfer in the unswitched state, the design parameters must be chosen with care. The reason was discovered in a later paper [10]; this showed that a particular relation between the coupling and dephasing variations was required to obtain low crosstalk, because it minimised coupling between the normal modes of the structure by maintaining a constant separation between their propagation constants.

In this paper we extend the approach of [10] in a systematic comparison of four mode evolution coupler designs that appear to allow good performance without excessive length, with parameters suitable for silica-on-silicon. The analysis is performed using weak coupled mode theory, in which the physical device shapes are abstracted into suitable variations of the coupling and dephasing parameters.

II. COUPLED MODE ANALYSIS

To analyse the structure, we first construct a suitable theoretical model. In the geometry studied here, we shall consider a coupler consisting of two waveguides with tapered width and gap, leading to a taper in velocity mismatch and in the variation of the coupling coefficient as shown in Figure 1. The variation of the former is antisymmetric, while that of the latter is symmetric. Propagation is assumed to take place mainly in the z-direction.

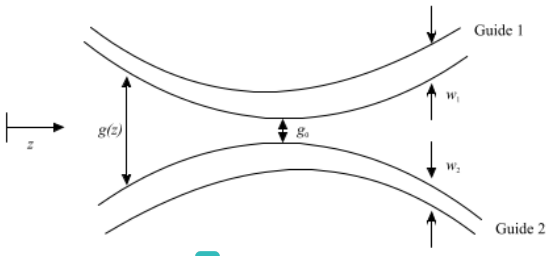

Figure 1. Geometry of a coupler with tapered velocity and tapered coupling; w_1 and w_2 are the widths of the two guides, $g(z)$ is the inter waveguide gap and g_0 is its lowest value.

We assume that both guides are weakly guiding and single moded; the widths and separation of the two guides vary slowly and gradually, so that the mode amplitudes also vary slowly with distance and weak coupled mode analysis can be used. To describe the power transfer process, approximate coupled mode equations defining the change in the mode amplitudes for two guides can be written in compact matrix-vector form as [7] :

$$\frac{d\overline{A}}{dz} = -j\overline{M}\,\overline{A} \qquad (1)$$

where $\overline{A} = \{A_1, A_2\}^T$ is a vector representing the amplitudes of the modes in the isolated guides 1 and 2, and $\overline{M}$ is a 2x2 matrix defined by :

$$\overline{M} = \begin{bmatrix} \Delta\beta & K \\ K & -\Delta\beta \end{bmatrix} \qquad (2)$$

Here, $\Delta\beta$ is the mismatch between the propagation constant of each waveguide relative to a mean value β_0, and K is the coupling coefficient. All parameters are a function of distance z. A solution to Equation (1) is now attempted in the form of summation of the normal modes of the structure in the limit of adiabatic variation, as:

$$\overline{A} = \overline{V}\exp(-j\int_0^z \overline{\Gamma}dz)\overline{C} \qquad (3)$$

here $\overline{C} = \{C_1, C_2\}^T$ is a vector containing the amplitudes of the two local eigen-modes, $\overline{V}$ is a 2x2 matrix containing the local normalised eigenvectors $\overline{v}_1$ and $\overline{v}_2$ arranged in columns, and $\overline{\Gamma}$ is a diagonal matrix of the corresponding eigenvalues γ_1 and γ_2.

If this is done, Equation (1) can be rewritten to give alternative coupled mode equations that now describe power transfer between the two eigenmodes of the complete structure rather than the modes of the isolated guides, as in [10]:

$$\frac{dC_1}{dz} = -(\overline{v}_1 \cdot \frac{d\overline{v}_2}{dz})\exp\{+j\int_0^z (\gamma_1 - \gamma_2)dz\}C_2$$
$$\frac{dC_2}{dz} = -(\overline{v}_2 \cdot \frac{d\overline{v}_1}{dz})\exp\{-j\int_0^z (\gamma_1 - \gamma_2)dz\}C_1 \qquad (4)$$

Now, consider the full power transfer condition, and ask how we should choose the spatial variations of $\Delta\beta$ and K, to restrict mode conversion

as far as possible. One way to do this is to set the dephasing term $(\gamma_1-\gamma_2)$ to the maximum value allowed by the system, since this makes the exponential terms in Equation (4) vary rapidly with distance, and hence implies that amplitude contributions coupled from one eigenmode to the other do not combine coherently to yield significant overall power transfer. This can be done by putting [10]:

$$\gamma_1=\sqrt{\mathrm{K}^2+\Delta\beta^2}=-\gamma_2=\mathrm{K}_o \tag{5}$$

where K_o is a constant dependent on the particular waveguide system, so that :

$$\gamma_1-\gamma_2=2\mathrm{K}_o \tag{6}$$

If this is done, we may write the coupling and dephasing terms as trigonometric functions of the form:

$$\begin{aligned}\mathrm{K}&=\mathrm{K}_o\sin(\theta)\\ \Delta\beta&=\mathrm{K}_o\cos(\theta)\end{aligned} \tag{7}$$

where θ is a new variable. It should be noted that K_o and $\Delta\beta$ are now no longer independent, so that the problem is less open-ended than before [13]. With this notation, the local eigenvectors can now be written as :

$$\begin{aligned}\bar{v}_1&=\left\{\cos(\frac{\theta}{2}),\sin(\frac{\theta}{2})\right\}^T\\ \bar{v}_2&=\left\{\sin(\frac{\theta}{2}),-\cos(\frac{\theta}{2})\right\}^T\end{aligned} \tag{8}$$

Equation (8) shows clearly that the eigenvectors are orthogonal to each other and effectively transform as they propagate through the structure by rotation, at a rate determined by the variation of the angle θ with distance.

For full power transfer (say) from a launch in Guide 1 to an output from Guide 2, the vector $\bar{v}_1$ must evolve from $\{1,0\}^T$ to $\{0,1\}^T$ through the length L of the device. Consequently, the structure should have boundary conditions of $\theta=0$ at $z=0$ and $\theta=\pi$ at $z=L$.

Differentiating Equation (8) and taking dot products, it is simple to show that the central coefficients in Equation (4) become:

$$\bar{v}_1\cdot\frac{d\bar{v}_2}{dz}=\frac{1}{2}\frac{d\theta}{dz}=-\bar{v}_2\cdot\frac{d\bar{v}_1}{dz} \tag{9}$$

so that Equation (4) itself reduces to:

$$\begin{aligned}\frac{dC_1}{dz}&=-\frac{1}{2}\frac{d\theta}{dz}\exp(+2j\mathrm{K}_o z)C_2\\ \frac{dC_2}{dz}&=\frac{1}{2}\frac{d\theta}{dz}\exp(-2j\mathrm{K}_o z)C_1\end{aligned} \tag{10}$$

Equations (10) imply that the term $\frac{1}{2}\frac{d\theta}{dz}$, which we term the 'shape function' of the device, is in fact a coupling coefficient between the eigenmodes, while the term $\pm 2\mathrm{K}_o$ is a dephasing parameter. Furthermore, the use of Equation (6) renders this parameter both constant and large.

It is well known from prior coupled mode analysis of directional couplers and grating filters [3][14], that there exists a Fourier-transform like relation between the spatial variation of the coupling coefficient $\mathrm{K}(z)$ and the dephasing length $\Delta\beta L$ (although this is strictly valid only in the limit of very weak coupling). By analogy we may see from Equation (10) that there will also be a Fourier-transform like relation between the shape function and the value of the coupling length $\mathrm{K}_o L$. Suitable shape functions may therefore be selected from the set of window functions used to obtain low sidelobes in conventional signal processing problems, subject to the additional constraint that they must be realisable in a physical device like a coupler using a positive coupling coefficient variation only [10]. This restriction does not apply in the case of a grating device, since the phase of the grating fringes may vary.

A number of different filter window functions are known to exist. These are conventionally optimised against particular design criteria (sidelobe level, passband ripple, etc), but have not been developed by a systematic and unified procedure. The most useful are the raised cosine, Hamming, Blackman, Kaiser, and Dolph-Chebyshev functions. In this case we consider the first three, together with a simple rectangle function. Each is known to give good sidelobe suppression, and is thus potentially suitable for our application, although slightly different performance is to be expected here due to

the requirement for strong coupling in a practical device, for reasons of high efficiency. Forms of these functions that achieve the correct initial and final values of θ over the range $0 \le z \le L$ are then given by [10][15] :

$$\frac{1}{2}\frac{d\theta}{dz} = \frac{\pi}{2L}$$ rectangle

$$\frac{1}{2}\frac{d\theta}{dz} = \frac{\pi}{2L} - \frac{\pi}{2L}\cos\left(\frac{2\pi z}{L}\right)$$ raised cosine

$$\frac{1}{2}\frac{d\theta}{dz} = \frac{\pi}{2L} - \frac{0.852\pi}{2L}\cos\left(\frac{2\pi z}{L}\right)$$ Hamming (11)

$$\frac{1}{2}\frac{d\theta}{dz} = \frac{\pi}{2L} - \frac{1.19\pi}{2L}\cos\left(\frac{2\pi z}{L}\right) + \frac{0.19\pi}{2L}\cos\left(\frac{4\pi z}{L}\right)$$ Blackman

In each case, the function is non-zero only within the device length, falling to zero outside. Figure 6.2(a) shows the variation of all four functions. Clearly the rectangle function has the most abrupt transition at the input and output; the other three functions are smoother, with the Blackman being the smoothest overall at the input and output but reaching the highest peak.

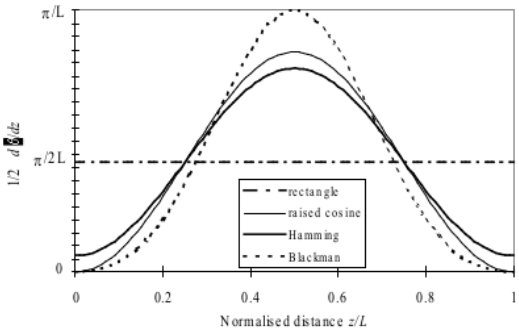

(a)

Figure 2 (a) Variation of the window functions $\frac{1}{2}\frac{d\theta}{dz}$ with normalised distance for each of the four expressions in Equation (11)

Equations (11) can obviously be integrated between the input of the device and an arbitrary point z to find the corresponding variations of θ with distance, which we term the 'rotation functions', as :

$$\theta = \frac{\pi z}{L}$$ rectangle

$$\theta = \frac{\pi z}{L} - 0.5\sin\left(\frac{2\pi z}{L}\right)$$ raised cosine

$$\theta = \frac{\pi z}{L} - 0.426\sin\left(\frac{2\pi z}{L}\right)$$ Hamming (12)

$$\theta = \frac{\pi z}{L} - 0.5952\sin\left(\frac{2\pi z}{L}\right) + 0.0476\sin\left(\frac{4\pi z}{L}\right)$$ Blackman

Figure 2 (b) shows the variation of these functions with normalised distance z/L. In each case, the initial and final values of θ are as required by the boundary conditions. However, as can be seen, the rectangle window function gives rise to a linear rotation function, while the other three all generate S-shaped variations, with a smoother transition at the input and output of the device and more rapid variation near the centre of the device.

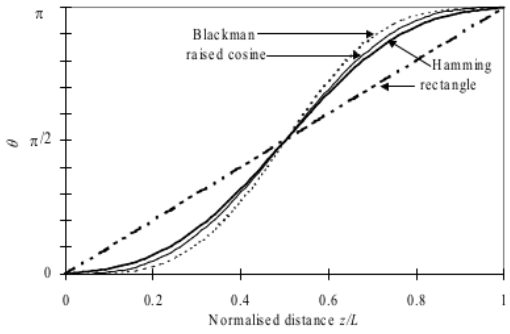

(b)

Figure 2(b). Variation of the rotation function θ with normalised distance for each of the four expressions in Equation (12).

III. NUMERICAL RESULTS

Equation (7) can then be used to calculate the corresponding variation of K and $\Delta\beta$. Figure 3 shows the variation of the normalised coupling coefficient K/K_o and the normalised dephasing term $\Delta\beta/K_o$ with distance, for each of the four window functions.

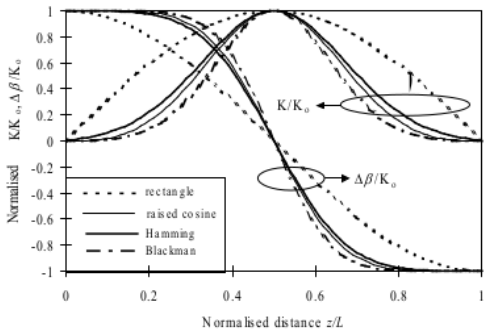

Figure 3. Variation of the normalised coupling coefficient and dephasing term with normalised distance, for rectangle, raised cosine, Hamming and Blackman window functions.

In each case, the variation of the coupling coefficient is approximately Gaussian, with a peak at the midpoint of the device where the gap is smallest. The dephasing function is antisymmetric, passing through zero at the device centre. It is also quasi linear near the device centre; however there are significant departures from linearity at the ends, where the variations become roughly constant. These characteristics are similar to the previous design which had used a parabolic variation in gap and a linear taper in width with distance [7]; however, it is now clear that there is a simple relationship between the peak value of the coupling coefficient and the slope of the dephasing variation near the device centre.

IV. POWER TRANSFER

Because no analytic solutions have yet been found to Equation (10), to simulate the effect of the different window functions on the power transfer characteristics of the device we have solved equations (10) by using a fourth order Runge-Kutta method to integrate each separate first-order equation along the propagation length L, subject to the boundary conditions $C_1 = 1$, $C_2 = 0$ at $z = 0$, for different values of the normalised coupling length K_oL. We then converted the amplitudes $C_{1,2}$ of the eigenmode into the corresponding isolated modal amplitudes $A_{1,2}$, and then converted these into modal powers as $P_{1,2} = A_{1,2}.A^*_{1,2}$. On integration of the differential equations, it was found that power was conserved to an accuracy of $\approx 0.0122\%$, with a moderate step size along the device length.

It is important to notice that the result obtained is dependent on the product of K_oL, and that the amount of power coupled between the guides may vary from close to zero to 100 %, depending on the choice of this parameter. Importantly, 100 % power transfer is obtained merely when K_oL is sufficiently large, and not for a particular value of K_oL (as in a conventional coupler). This improves the device's tolerance to fabrication variations, since K_o need no longer be fixed at a precise value.

Figure 4 shows the variation of normalised power with normalised distance z/L for the four window functions, assuming a fixed value of $K_oL = 10$ (large enough for full power transfer). In each case, the straight-through power P_1 gradually falls, while the cross-coupled power P_2 rises. A large ripple appears for the rectangle function, which disturbs the shape of the power transfer characteristics, and causes a finite degree of crosstalk. However, this ripple decreases in amplitude and increases in frequency as K_oL becomes large.

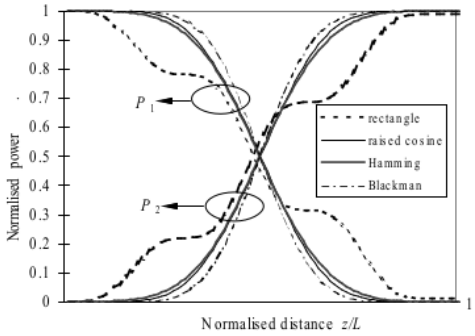

Figure 4. Power variation in the two guides with normalised distance z/L, for the different window functions given in Equation (12).

The oscillation suggest that some beating must occur between the two normal modes. However, by using the raised cosine, Hamming or Blackman window functions, the ripples can be largely eliminated and much smoother power transfer characteristics are achieved. It was verified that very similar results are obtained if the integration is carried out over the reduced range of $0.05 \le z/L \le 0.95$, showing that the desired mode evolution

behaviour can indeed be achieved using a practical device with a finite guide separation.

Figure 5 now shows the variation of the straight-through output power $P_1(L)$ with normalised coupling length K_oL. As the coupling length rises, the straight through power gradually falls, indicating a rise in the cross-coupled power. However, for the rectangle window function, significant sidelobes appear, which can result in large crosstalk for a poor choice of K_oL. This is unfortunate, since our aim is to relax fabrication tolerances. However, when the raised cosine, Hamming, and Blackman functions are used, the sidelobe levels are considerably lower throughout, suggesting that lower values of K_oL will be needed to obtain low crosstalk with these design.

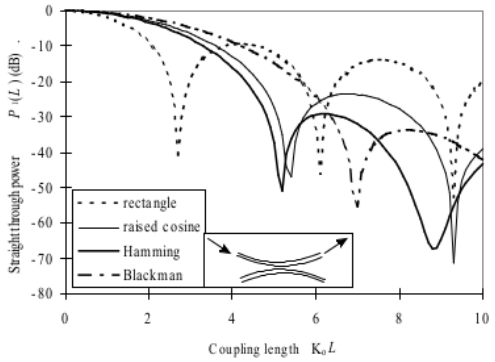

Figure 5.. Variation of the straight through output power $P_1(L)$ with normalised coupling length K_oL

These functions also show a smooth power transfer. The worst sidelobe level obtained using the rectangle function was -9.35 dB for a full length device, and -8.81 dB for a reduced length structure. However, it is clear that by using the more sophisticated raised cosine, Hamming, and Blackman functions, the worst-case sidelobe level can be reduced but at the expense of increased device length. Among these window functions, the Hamming function gives a good compromise between the sidelobe level and device length. Its maximum sidelobe level is -29.16 dB, which is more than a 19 dB reduction over the rectangle function and over 5 dB compared to the raised cosine function. This benign characteristic of the Hamming function was also found previously for a slightly different problem involving non-uniform holographic gratings [14]. However the best sidelobe level overall is obtained using the Blackman function. This give more than 24 dB reduction over the rectangle window function, but with a longer normalised coupling length

V. CONCLUSION

An analysis of mode evolution couplers has been performed using weak coupled mode theory. It has been shown that overall performance may be improved by appropriate choices of the coupling and dephasing variations, which follow from particular window functions that induce gradual rotation of the eigenmode shape in phase space. Excellent performance can be obtained using a Blackman window function, but only at a price of greatly increase length. The alternative Hamming shape function appears to give the best compromise between performance and length.

REFERENCES

1. R. V. Schmidt, R. C. Alferness, "Directional coupler switches, modulators, and filters using alternating □□ techniques", IEEE Trans. Circuit. Syst,. vol. CAS-26, 1099-1108, 1979.
2. M.G.F. Wilson, G.A. Teh, "Tapered optical directional coupler", IEEE Trans. on Microwave Theory and Tech., vol. MTT-23, 85-92, 1975.
3. R.C. Alferness, P.S. Cross, "Filter characteristics of codirectionally coupled waveguides with weighted coupling", IEEE Journal of Quantum. Electron., vol. QE-14, 843-847, 1978.
4. T. Findakly, C.L. Chen, "Optical directional couplers with variable spacing", Appl. Opt., vol. 17, 769-773, 1978.
5. R.V. Ramaswamy, H. S. Kim, "A novel tapered, both in dimension and in index, velocity coupler switch", IEEE Photon. Tech. Lett., vol. 5, 557-560, 1993.
6. A.F. Milton, W.K. Burns, " Mode coupling in tapered optical waveguide structures and electro-optics switch", IEEE Trans. on Circuits and Syst., vol. CAS-26, 1020-1028, 1979.
7. R.R.A. Syms, R.G. Peall, "The digital optical switch: Analogous directional coupler devices", Opt. Comm., vol. 69, 235-238, 1989.
8. Y. Silberberg, P. Perlmutter, and J. Baran, "Digital optical switch", Appl. Phys. Lett., vol. 51, 1230-1232, 1987.
9. S. Xie, H. Heidrich, D. Hoffmann, H-P. Nolting and F. Reier, "Carrier-injected GaInAsP/InP directional coupler optical switch with both tapered velocity and tapered coupling", IEEE Photon. Tech. Lett., vol. 4, 166-169, 1992.

10. R.R.A Syms, " The digital directional coupler : improved design", IEEE Photon. Tech. Lett., vol. 4, 1135-1138, 1992.
11. R. Pregla, A. Pascher, "The method of lines", in Numerical techniques for microwaves and millimeter passive structures, Itoh T., Chapter 6, 381-446, Wiley, New York, 1989.
12. J. Gerdes , R. Pregla, "Beam-propagation algorithm based on the method of lines", J. of Opt. Soc. of Am. B, vol. 8, 389-394, 1991.
13. A. Syahriar, V.M. Schneider, S.J. Al-Bader, "The design of mode evolution couplers", IEEE J. Lightwave. Technol., vol. LT-16, October 1998.
14. H. Kogelnik, "Filter response of non-uniform almost periodic structures", Bell Syst. Tech. J., vol. 55, 109-126, 1976.

ANALYSIS OF TAPERED VELOCITY AND TAPERED COUPLING COUPLERS

ORIGINALITY REPORT

8%	4%	7%	0%
SIMILARITY INDEX	INTERNET SOURCES	PUBLICATIONS	STUDENT PAPERS

PRIMARY SOURCES

1	media.neliti.com Internet Source	2%
2	www.osapublishing.org Internet Source	1%
3	R. R. A. Syms. "Improved coupled-mode theory for codirectionally and contradirectionally coupled waveguide arrays", Journal of the Optical Society of America A, 1991 Publication	1%
4	S. Xie, H. Heidrich, D. Hoffmann, H.-P. Nolting, F. Reier. "Carrier-injected GaInAsP/InP directional coupler optical switch with both tapered velocity and tapered coupling", IEEE Photonics Technology Letters, 1992 Publication	1%
5	K. Kishioka. "A design method to achieve wide wavelength-flattened responses in the directional coupler-type optical power splitters", Journal of Lightwave Technology, 2001	<1%

Publication

6	Syms, R.R.A.. "The digital optical switch: analogous directional coupler devices", Optics Communications, 19890101 Publication	<1%
7	Ary Syahriar. "A simple analytical solution for loss in S-bend optical waveguide", 2008 IEEE International RF and Microwave Conference, 2008 Publication	<1%
8	Chi-Feng Chen, Yun-Sheng Ku, Tsu-Te Kung. "Design of short length and C+L-band mismatched optical coupler with waveguide weighted by the Blackman function", Optics Communications, 2009 Publication	<1%
9	M. Raburn, Bin Liu, K. Rauscher, Yae Okuno, N. Dagli, J.E. Bowers. "3-D photonic circuit technology", IEEE Journal of Selected Topics in Quantum Electronics, 2002 Publication	<1%
10	Vitor Marino Schneider, Haroldo T. Hattori. "Wavelength insensitive asymmetric triple mode evolution couplers", Optics Communications, 2001 Publication	<1%

J. Marti, D. Pastor, M. Tortola, J. Capmany, A.

11	Montero. "On the use of tapered linearly chirped gratings as dispersion-induced distortion equalizers in SCM systems", Journal of Lightwave Technology, 1997 Publication	<1%
12	www.research-collection.ethz.ch Internet Source	<1%
13	Harold T. Stokes, Branton J. Campbell, Dorian M. Hatch. "Order parameters for phase transitions to structures with one-dimensional incommensurate modulations", Acta Crystallographica Section A Foundations of Crystallography, 2007 Publication	<1%
14	Chang, Hung-chun, Je-Hsiung Lan, Mark A. Mentzer, Song-Tsuen Peng, Henry J. Wojtunik, and Ka K. Wong. "", Integrated Optics and Optoelectronics, 1990. Publication	<1%
15	Maxim Y. Greenberg, Meir Orenstein. "Simultaneous Dual Mode Add Drop Multiplexer for Optical Interconnects Buses", Integrated Photonics Research and Applications/Nanophotonics for Information Systems, 2005 Publication	<1%
16	Gia-Wei Chern. "Analysis and Design of Almost-	

Periodic Vertical-Grating-Assisted Codirectional Coupler Filters with Nonuniform Duty Ratios", Applied Optics, 09/01/2000

Publication

<1%

Exclude quotes	On	Exclude matches	Off
Exclude bibliography	On		